Aalborg Universitet

AALBORG UNIVERSITY

DENMARK

Harmonic Issues Assessment on PWM VSC-Based Controlled Microgrids using Newton Methods

Agundis-Tinajero, Gibran; Segundo-Ramirez, Juan; Peña-Gallardo, Rafael; Visairo-Cruz, Nancy; Nuñez-Gutierrez, Ciro; Guerrero, Josep M.; Savaghebi, Mehdi

Harmonic Issues Assessment on PWM VSC-Based Controlled Microgrids using Newton Methods

Gibran Agundis-Tinajero, *Student Member, IEEE,* Juan Segundo-Ramírez, *Member, IEEE,* Rafael Peña-Gallardo, *Member, IEEE,* Nancy Visairo-Cruz, *Member, IEEE,* Ciro Núñez-Gutiérrez, *Member, IEEE,* Josep M. Guerrero, *Fellow, IEEE,* Mehdi Savaghebi, *Senior Member, IEEE.*

Abstract—This paper presents the application of Newton-based methods in the time-domain for the computation of the periodic steady state solutions of microgrids with multiple distributed generation units, harmonic stability and power quality analysis. Explicit representation of the commutation process of the power electronic converters and closed-loop power management strategies are fully considered. Case studies under different operating scenarios are presented: grid-connected mode, islanded mode, variations in the Thevenin equivalent of the grid and the loads. Besides, the close relation between the harmonic distortion, steady state performance of the control systems, asymptotic stability and power quality is analyzed in order to evaluate the importance and necessity of using full models in stressed and harmonic distorted scenarios.

Index Terms—Commutation process, harmonics, limit cycle, microgrid, Newton methods, periodic steady state, power management, pulse-width modulation, voltage source converter.

I. INTRODUCTION

IN order to ensure the safe, reliable and controlled operation of the microgrid (MG) system, it is necessary to carry-out model-based studies for design purposes, monitoring, control, and network reconfiguration, etc. Some of these studies are run in transient state and others in steady state; nonetheless, for any of these scenarios are needed efficient mathematical models and computational algorithms for execution and analysis. In particular, the steady state solution of an MG system is necessary to carry out studies such as power quality, stability, design of components, power flow, robustness, among others; however, despite that in conventional power systems the analysis previously mentioned are well established [1], during the design stage of the MG, the computation of the steady state solution represents a challenging task due to the incorporation of power electronic converters, nonlinear loads and closed-loop control systems.

On the other hand, the assumption of balanced and perfectly sinusoidal three-phase voltage and current waveforms are conditions increasingly difficult to sustain as valid in stressed and harmonic distorted scenarios, since harmonic generation, unbalance, interaction of control and harmonic components, resonances, etc, are phenomena commonly found in systems with high penetration of distributed generation units such as microgrids [2], [3]. This could result, in practice, in erroneous

Gibran Agundis-Tinajero, Juan Segundo-Ramírez, Rafael Peña-Gallardo, Nancy Visairo-Cruz and Ciro Núñez-Gutiérrez are with the Universidad Autónoma de San Luis Potosí, San Luis Potosí, S.L.P., México.

Josep M. Guerrero and Mehdi Savaghebi are with the Aalborg University, Aalborg, 9200 Denmark.

or unfavorable operating scenarios overlooked in the design and evaluation stages [1], [4], [5]. In this way, this gap has been recognized and recently addressed in the open literature, albeit incipient. For instance, reference [6] proposed a control system for regulating the grid power flow and for the reduction of the grid current total harmonic distortion in presence of nonlinear loads; however, the control is based on average models and therefore, it does not include the harmonic interaction with the power network. Reference [7] presents a hierarchical control; however, the voltage source inverter (VSI) used in this work are modeled based only on their control functions so that fast switching transients, harmonics, and inverter losses are neglected. In [8] a control strategy based in droop control is proposed; nevertheless, the control is tested in a small signal model and, furthermore, in order to reduce the system equations, the fast dynamics are neglected and the dc/dc converter is assumed to be a controllable voltage source. To analyze the harmonic stability of balanced AC power-electronic-based systems, an approach based on impedance is proposed in [9], this approach considers the harmonic content as a disturbance matrix. In [10], the authors derive conditions for stability of droop controlled microgrids; however, these conditions of stability are tied to several assumptions increasingly difficult to achieve in realistic systems with high penetration of DG units with power electronic interfaces, for example, the authors model the inverters as AC voltage sources, assume constant impedance load models, only the fundamental component of voltages and currents are considered, among others.

It is important to notice that, in the previous contributions, the full relationship harmonics-asymptotic stability has been overlooked; however, this problem has been addressed in [11], [12] for adjustable speed drive systems and dynamic voltage restorer, respectively, and more recently in [9] for ac power electronic-based power system but using average models. Furthermore, it has been found that, in microgrids, the variables of control and the grid are coupled and do exist an interaction between them [9], [13], such that, there are effects of the harmonic distortion on the performance of the control systems and the stability of the periodic solution, and vice versa, that must be taken into account. In regards to the aforementioned, there is a close relationship among control systems, harmonics, asymptotic stability, transient and steady state performance that must be considered in microgrid design and studies in order to not overlook phenomena or undesirable behaviors when using inappropriate models or analysis techniques [14].

In this way, this paper presents the performance assessment of the fast-time domain methods for the computation of the periodic steady state solutions of MGs, and shows the potential applications of these methods to study the intrinsic relationship among harmonics, asymptotic stability, control and the MG without resort to simplifications of the used models that could compromise the reliability of the analyses. In addition, this paper tries to bring out the existing gaps on stability and power quality analyzes of harmonic distorted and controlled microgrids through some basic case studies.

This paper is organized as follows: Section II presents the methodologies used to compute the periodic steady state solutions of MG systems. Section III describes the general formulation of the fast-time domain methods. The test microgrid, the close-loop controls and the validation state-space MG model against a professional time domain simulation program are given in Section IV. The performance assessment of the fast-time domain methods for computation of the periodic steady state solutions of MGs is given in Section V. Using the top performer fast-time domain method found in the previous Section, harmonic stability and power quality analyzes are performed in Section VI.

II. ON THE COMPUTATION OF THE PERIODIC STEADY STATE SOLUTION

A common and straightforward practice in the time domain to compute the periodic steady state solution of a MG system is to simulate over several full cycles until the initial transient dies out. This technique is known as Brute Force method (BF) [15]; EMTP-type programs fall within this category. These professional programs rely on the Dommel's formulation [16], for example PSCAD/EMTDC, EMTP-RV, RSCAD, ATP-EMTP, among others. However, this conventional time-domain process presents some drawbacks for poorly damped, unstable, or stiff systems. Firstly, the BF method can only compute stable periodic solutions if the initial condition $\mathbf{x_0}$ is in the neighborhood U of the attractor of the limit cycle X (i.e., $X \subset U$). Therefore, the computation of unstable periodic steady state solution is not readily available using EMTP-type simulators. Assuming a stable limit cycle X and a good initial condition ($\mathbf{x_0} \in U$), the BF method has to be applied over a large number of cycles and with small time steps in poorly damped and stiff systems, respectively; both cases increase the computational effort. Detailed MG models are usually stiff and present stability problems and poorly damped scenarios if the controllers are not properly tuned, designed or implemented [17]. Therefore, even with a stable limit cycle and a good initial condition, the computation of the periodic steady state solution of MG's using the BF method may take a very large computational effort if the full harmonic interactions, the closed-loop controls and the harmonic cross-coupling need to be explicitly considered.

In order to overcome this problem, EMTP-type programs can perform a load-flow initialization; the load-flow solution is based on algebraic constraints, i.e., sources are replaced by PQ, PV or slack bus constraints, loads are replaced by PQ constraints and all network components must provide a load-flow solution model [18]. Despite that this initialization becomes complex when non-linear components and/or power electronics switching devices are used, the EMTP-type programs perform the initialization using mean-value models and then change to switched models after establishing the steady-state operating condition; however, it is worth mentioning that fully automatic methods to initialize a nonlinear switched system with close-loop controls are still under development [18]. It is important to highlight that even though the features offered by the EMTP-type programs, several analyses such as design of components, optimization, stability, control design, among others, typically rely on state-space representation of the system. Therefore, efficient numerical methods for state-space models of microgrids are required [19].

One way to compute the steady state solution of microgrids represented by a set of autonomous ordinary differential equations, i.e., $\dot{\mathbf{x}} = \mathbf{f}(\mathbf{x})$, is simply to solve $\mathbf{f}(\mathbf{x}) = 0$. Average models fall within this type of systems, but they have evident limitations to evaluate adverse effect of the harmonic distortion on the performance of the MG. Alternatively, the harmonic domain modeling approach is able to consider the distorted nature of microgrids and also leads to time-invariant representations; however, the proper modeling of closed-loop controls and nonlinearities are still a bottleneck in this domain [20]. In order to deal with these problems, the fast time-domain methods were proposed [21], [22] and based on these seminal papers, other methods have been proposed and some of them will be presented in the following sections. Depending on the kind of system, these techniques are referred as shooting methods, Poincaré map methods or simply Newton methods [15]; in particular for non-autonomous systems, the shooting and the Poincaré map methods are essentially the same. In addition to the computation of the periodic solution, these methods also give information about the asymptotic stability of the computed steady-state solution.

The fast time-domain methods also present convergence problems with power electronic-based systems including closed-loop controls. Basically, the source of the convergence problems is the numerical integration during the commutation process of the power electronic converters. In the case of using nonlinear models of the semiconductor switches, very small time steps are needed during the switching transition, becoming prohibitive the computation time. This approach is useful and necessary if the switching phenomena want to be analyzed; however, from the power systems perspective, it is more important the harmonic interaction among the different components, elements and systems of the power grid than the intrinsic phenomena of the commutation of the semiconductor devices; nevertheless, to overcome this convergence issue of the fast time-domain methods, in [11], [12] the authors propose a model for the voltage source converter (VSC) that avoid the convergence problems for electronic-based systems and therefore this VSC model is used in this paper.

In the next Section the general formulation of the fast time-domain methods is presented.
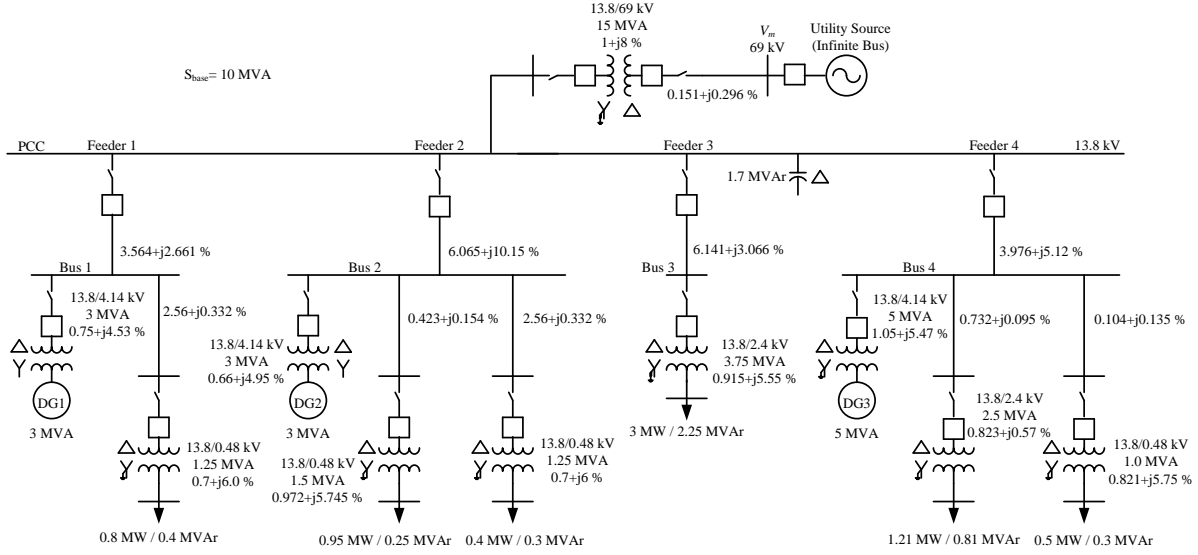
Fig. 1. Single line diagram of the microgrid.

III. NEWTON METHODS

In general, the mathematical model of periodic switched nonlinear electric power systems can be given by the following ordinary differential equation set,

$$\dot{\mathbf{x}} = \mathbf{f}(t, \mathbf{x}) \tag{1}$$

where $\mathbf{x}$ is the state vector of n elements.

The periodic steady state solution of (1) has a fundamental period T, such that the following relation is satisfied in steady state,

$$\mathbf{x}_T = \mathbf{x}_0 \tag{2}$$

where $\mathbf{x}_0$ is the state vector at t_0 and $\mathbf{x}_T = \mathbf{x}(t_0 + T, t_0; \mathbf{x}_0)$; for simplicity t_0 can be set equal to zero. Besides, the representation of dynamical periodic systems can be performed by using a Poincaré map $\mathbf{P}(\mathbf{x})$. Thereby, (2) can be written as follows,

$$\mathbf{x}_T = \mathbf{P}(\mathbf{x}_0) \tag{3}$$

Then, this problem can be solved through an iterative Newton method,

$$\mathbf{x}_0^{i+1} = \mathbf{x}_0^i - \left(\left. \frac{\partial \mathbf{P}(\mathbf{x}_0)}{\partial \mathbf{x}_0} \right|_{\mathbf{x}_0 = \mathbf{x}_0^i} - \mathbf{I} \right)^{-1} \left(\mathbf{P}(\mathbf{x}_0^i) - \mathbf{x}_0^i \right) \tag{4}$$

The periodic steady state solution is found once two consecutive state vectors meet a convergence criterion error. Also, the state transition matrix $\mathbf{\Phi}$ can be defined as,

$$\mathbf{\Phi} = \left. \frac{\partial \mathbf{P}(\mathbf{x}_0)}{\partial \mathbf{x}_0} \right|_{\mathbf{x}_0 = \mathbf{x}_0^i} \tag{5}$$

It should be noticed that the eigenvalues of $\mathbf{\Phi}$ are the Floquet multipliers [23]; therefore, the transition matrix of the computed solution (4) can be used to obtain the stability of the periodic solution of the system [15], i.e. if all the Floquet multipliers are inside the unit circle in the complex plane Z the system is stable, otherwise unstable.

Several methods have been developed to compute $\mathbf{\Phi}$ [20], and all those methods rely on numerical integration processes. Each method differs from each other on how the approximation is done, and in the number of full cycles required for the full identification of $\mathbf{\Phi}$. In [22] the Aprille and Trick method (AT) was proposed, and the identification of $\mathbf{\Phi}$ requires only the integration of one full cycle and the computation of the Jacobian of (1) along the trajectory $\mathbf{x}(t, t_0; \mathbf{x}_0^i)$ for $t_0 \leqslant t \leqslant t_0 + T$. Later, based on the Poincaré map approach, the Numerical Differentiation (ND) and Direct Approach (DA) methods were proposed [24]. In both, the computation of $\mathbf{\Phi}$ is done column-by-column requiring the integration of $n + 1$ full cycles.

The ND approach is based in the perturbation of the n state variables of (1), while DA is based on the linearized version of (1) around an orbit started at $\mathbf{x}_0^i$. In [25], the Enhanced Numerical Differentiation (END) method was proposed to take advantage of the half-wave symmetry of waveforms of practical power systems and compute $\mathbf{\Phi}$ similarly to the ND method, but only with the integration of $(n+1)/2$ full cycles, leading to improve the computation time but with a lower accuracy of $\mathbf{\Phi}$. At the same time, in [26] a Discrete Exponential Expansion (DEE) method was proposed, following an identification procedure step-by-step based on a recursive formulation that requires the integration of only one full cycle. Additionally, the Finite Differences (FD) method [15] is an alternative technique in the time-domain formulated in terms of a set of difference equations. One of the main advantages of this method over the others is the explicit trajectory of the periodic solution of each state variable, but the main drawback is the large number of algebraic equations to be solved at each Newton iteration.

IV. MICROGRID SYSTEM

Figure 1 shows the single line diagram of the microgrid used as test system. Its mathematical model including the

control system has 86 ordinary differential equations for grid-connected mode and 83 for islanded mode. The system configuration, parameters and control scheme were extracted from [27], [28]. This power system is widely used for studies in microgrids, such as, faults events analysis [29], small signal analysis [30], sensitivity analysis [28], among others. The MG has a nominal voltage of 13.8 kV and it is connected through a transformer to a harmonic free infinite bus (main grid) of 69 kV. The three distributed generation units include a voltage source converter [31] with a RL filter of $0.01 + j0.15\ p.u.$ and a frequency modulation index (m_f) of 21 (1260 Hz).

A. Pulse-width modulation (PWM)

The power electronic converter used in each DG unit is a three-phase two-level VSC. The AC terminal voltage behind the loss resistance is given by the following equation,

$$\begin{bmatrix} v_a(t) \\ v_b(t) \\ v_c(t) \end{bmatrix} = \begin{bmatrix} (S_a(t) - 1/3\sum_{i=a,b,c} S_i(t))v_{dc}(t) \\ (S_b(t) - 1/3\sum_{i=a,b,c} S_i(t))v_{dc}(t) \\ (S_c(t) - 1/3\sum_{i=a,b,c} S_i(t))v_{dc}(t) \end{bmatrix} \quad (6)$$

where $S_a(t)$, $S_b(t)$ and $S_c(t)$, are the switching functions for the phase a, b, and c, respectively. $v_{dc}(t)$ is the DC-side voltage of the VSC. For the purpose of this contribution, $v_{dc}(t)$ is considered constant but it can be time-varying or be described by another set of equations. The switching functions are modeled using an hyperbolic tangent approach introduced in [31] in order to avoid convergence problems of the Newton methods and numerical oscillations. The switching functions are modeled as follows,

$$S_i(t) \approx \frac{(tanh(\alpha(v_{si}(t) - tri(t))) + 1}{2} \quad (7)$$

where $v_{si}(t)$ is the control signal and $tri(t)$ is the sawtooth waveform, $i = a, b, c$. The parameter α is selected as,

$$\alpha = \frac{\Omega_c}{f_{sw}} \quad (8)$$

where f_{sw} is the switching frequency of the PWM modulation technique and Ω_c is the cutoff frequency of the VSC model. For this contribution, the bandwidth of each VSC (Ω_c) was selected as 15 times f_{sw}, and therefore $\alpha = 15$.

B. Power management strategies

Power management strategies (PMS) are required for the proper operation of microgrids with multiple DG units [28], particularly during the islanded operation mode. The PMS adopted for each DG unit of this microgrid is schematically shown in Fig. 2 [28]. Real and reactive power management blocks establish the real and reactive power output of each DG unit, respectively. The block of current controller and gate pulses take the outputs of the real and reactive power blocks and generate the reference voltage of the controlled VSC.
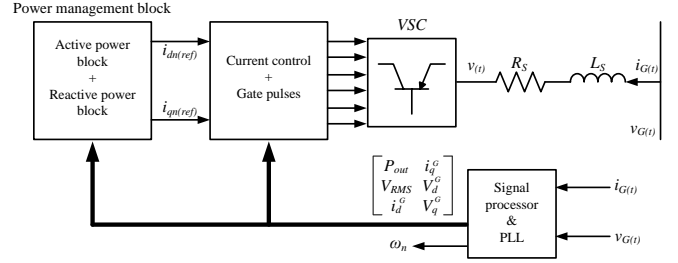

Fig. 2. Control block diagram.

C. Validation of the state-space model with PSCAD

Due that to perform the analysis of the controlled MG with the fast-time domain methods the state space representation is needed, the obtained state-space model (SSM) of the complete microgrid in the form (1) needs to be validated against the solutions of a professional software such as PSCAD [32]. Fig. 3 shows the three phase current flowing from the point of common coupling (PCC) bus to Bus 3. Please observe that both solutions are practically the same, despite the formulation of the dynamical model in PSCAD relies on the Dommel's method based on the trapezoidal rule [16], [33]. Furthermore, it can be seen that the current signals are highly distorted, this is caused because of a parallel resonance that increases the harmonic distortion on the MG system.
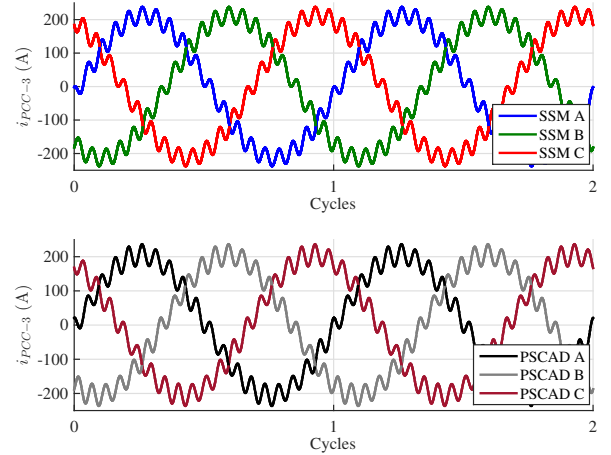
Fig. 3. Periodic steady state solution of the branch current from PCC to Bus 3 (i_{PCC-3}). (Top) Computed with the Newton method using the state-space model (SSM). (Bottom) Computed with PSCAD using the brute force (BF) approach.

V. PERFORMANCE ASSESSMENT OF THE FAST-TIME DOMAIN METHODS IN THE TEST MG SYSTEM

Two case studies of the microgrid under different operating conditions are presented in this Section. In the first case, the microgrid is interconnected to the main grid operating in periodic steady state, when suddenly is disconnected to operate in islanded mode. In the second case, the microgrid is in islanded mode in steady state, when the load of the feeder

3 (S_{L3}) is suddenly decreased from 3 MW / 2.25 MVAR to 0.6 MW / 0.42 MVAR.

The accelerated computation of periodic solutions for the case studies is carried out with the six Newton methods aforementioned (DEE, AT, FD, DA, ND and END), and the results obtained are compared to assess the advantages and disadvantages of each method. The convergence error tolerance used in the case studies is 1×10^{-8} and the state vector at the end of the 10th cycle is used for initialization of the Newton methods; the computation of this state vector is performed through numerical integration of (1) using as initial condition the state vector at $t = 0$ of the previous operating condition in steady state, i.e., grid-connected mode for the case study 1 and islanded mode with $S_{L3} = 3$ MW $+ j2.25$ MVAr for the case study 2. After the 10th cycle the Newton iterations begin and the convergence mismatches are given in multiples of the cycles that each method need to iterate, i.e., DEE, AT and FD methods require one full cycle, the ND and DA methods require $(n + 1)$ cycles and the END method requires $(n+1)/2$ cycles, where n is the number of ordinary differential equations of the system model. The case studies and methods were implemented in Matlab and the results verified with the professional software PSCAD.

A. Case study 1: disconnection from the main grid

Table I shows the relative efficiency of each method respect to the BF method to achieve the periodic steady state solution within the established tolerance. Besides, the maximum Floquet multiplier is calculated for each method. Notice that Φ is not computed in the BF and FD methods; therefore the Floquet multipliers cannot be calculated with those methods and neither the stability of the computed periodic solution. However, in this case, it is clear that the periodic steady state solution is stable since the BF method is able to reach it. It is important to remember that the six Newton methods are able to compute both stable and unstable periodic steady state solutions; this is a valuable feature since the unstable solution can become stable with the proper selection of the control gains or system parameters.

It can be seen that BF and DEE are the slowest and the fastest methods, respectively. DEE is around 68, 3.46, 3.46, 1.85, 1.83, and 1.79 times faster than BF, ND, FD, DA, AT and END, respectively. Observe that the maximum Floquet multiplier with each method (AT, ND, DA, END, and DEE) is computed and its value is inside the unit circle for all methods with standard deviation of 5.0438×10^{-4}.

Table II shows the results obtained in terms of the number of cycles required to obtain the periodic steady state solution and the Newton iterations are highlighted in gray. Observe in Table II that the BF method requires 5283 full cycles and reaches the periodic steady state with an error of 9.978×10^{-9}, while the DEE method requires 5 Newton iterations and the others methods require 3 Newton iterations. The END, DA, AT, ND, and FD methods have a quadratic convergence characteristic. Although the DEE method requires more iterations is also the fastest since the time to compute the transition matrix at each Newton iteration is less as compared with the others Newton methods.

TABLE I
COMPARISON BETWEEN CPU TIMES AND STABILITY IN CASE 1

Methods	CPU times (s)	Comparison between CPU times $\frac{T_{FB}}{T_{xx}}\big\|_{xx=FB,...,EED}$	Max. Floquet multiplier
BF	80007.10	1.00	N/A
ND	4056.70	19.72	0.9978
FD	4051.06	19.74	N/A
DA	2174.96	36.78	0.9978
AT	2152.25	37.17	0.9978
END	2094.94	38.19	0.9989
DEE	1169.95	68.38	0.9974

B. Case study 2: load change

Table IV shows the relative efficiency of each method. The BF and the DEE are the slowest and the fastest methods, respectively. For this case, the DEE method is around 67.05, 3.68, 3.67, 2.01, 1.99 and 1.93 times faster than BF, ND, FD, DA, AT and END, respectively.

Table III shows the results obtained in terms of the number of cycles required to obtain the periodic steady state solution and the Newton iterations are highlighted in gray. The BF method requires 4969 full cycles and reaches the periodic steady state with an error of 9.992×10^{-9}, while the DEE method requires 5 Newton iterations and the other methods require 3 Newton iterations, being the FD method the one that gets the smallest convergence error, i.e, 4.843×10^{-12}.

The first two case studies presented a comparison between the Newton and the BF methods; the Newton methods offer a suitable alternative to compute the periodic steady state solution of dynamical systems represented by full-order models, furthermore, they provide information about the asymptotic stability of the computed periodic steady state solution, except the FD method.

VI. FAST-TIME DOMAIN HARMONIC ASSESSMENT

In this Section the harmonic assessment of the microgrid is shown through three case studies using the DEE method and the professional software PSCAD. These case studies are presented in order to bring out the potential applications of the Newton methods and also to expose the relationship among harmonics, asymptotic stability, control and the network. The first two case studies are carried out with the microgrid operating in islanded mode and the last one in grid-connected mode. The DEE method is used because it is the fastest as demonstrated in the previous Section. Firstly, an analysis of the harmonic effects on the power losses and power quality is presented. Secondly, the harmonic interaction between the control system and the microgrid is analyzed. Finally, the harmonic effects on the asymptotic stability of the computed periodic solutions are analyzed. All case studies presented in the following sections are focused on the switching harmonics caused by the PWM inverters considering the nonlinear and cross-coupling interaction with the DG units, controllers and network elements and components; however, another harmonic sources, such as the background harmonics [13], [34], can be easily taken into account using the proposed fast-time domain methods.

TABLE II
MISMATCHES DURING CONVERGENCE OF THE METHODS IN CASE 1

Cycles	BF	DEE	AT	FD	DA	ND	END
1	5.217×10^{-3}	5.217×10^{-3}	5.217×10^{-3}	5.217×10^{-3}	5.217×10^{-3}	5.217×10^{-3}	5.217×10^{-3}
2	6.226×10^{-3}	6.226×10^{-3}	6.226×10^{-3}	6.226×10^{-3}	6.226×10^{-3}	6.226×10^{-3}	6.226×10^{-3}
⋮	⋮	⋮	⋮	⋮			
10	3.969×10^{-3}	3.969×10^{-3}	3.969×10^{-3}	3.969×10^{-3}	3.969×10^{-3}	3.969×10^{-3}	3.969×10^{-3}
11	3.843×10^{-3}	5.586×10^{-4}	2.224×10^{-5}	2.277×10^{-5}	⋮	⋮	⋮
12	3.729×10^{-3}	4.194×10^{-5}	5.594×10^{-8}	4.968×10^{-8}	⋮	⋮	⋮
13	3.623×10^{-3}	2.239×10^{-6}	5.465×10^{-12}	1.567×10^{-12}	⋮	⋮	⋮
14	3.524×10^{-3}	5.745×10^{-8}			⋮	⋮	⋮
15	3.431×10^{-3}	5.316×10^{-9}			⋮	⋮	⋮
⋮	⋮				⋮	⋮	⋮
52	1.502×10^{-3}				⋮	⋮	3.290×10^{-5}
⋮	⋮				⋮	⋮	⋮
94	1.100×10^{-3}				2.224×10^{-5}	2.309×10^{-5}	2.662×10^{-8}
⋮	⋮				⋮	⋮	⋮
136	2.110×10^{-3}				⋮	⋮	2.604×10^{-12}
⋮	⋮				⋮	⋮	
178	1.207×10^{-3}				5.538×10^{-8}	4.660×10^{-8}	
⋮	⋮				⋮	⋮	
262	5.484×10^{-4}				5.338×10^{-12}	5.479×10^{-12}	
⋮	⋮						
5283	9.978×10^{-9}						

TABLE III
MISMATCHES DURING CONVERGENCE OF THE METHODS IN CASE 2

Cycles	BF	DEE	AT	FD	DA	ND	END
1	9.094×10^{-3}	9.094×10^{-3}	9.094×10^{-3}	9.094×10^{-3}	9.094×10^{-3}	9.094×10^{-3}	9.094×10^{-3}
2	8.109×10^{-3}	8.109×10^{-3}	8.109×10^{-3}	8.109×10^{-3}	8.109×10^{-3}	8.109×10^{-3}	8.109×10^{-3}
⋮	⋮	⋮	⋮	⋮	⋮	⋮	⋮
10	1.365×10^{-3}	1.365×10^{-3}	1.365×10^{-3}	1.365×10^{-3}	1.365×10^{-3}	1.365×10^{-3}	1.365×10^{-3}
11	1.270×10^{-3}	3.815×10^{-4}	3.806×10^{-4}	3.806×10^{-4}	⋮	⋮	⋮
12	1.181×10^{-3}	1.157×10^{-5}	7.201×10^{-8}	7.158×10^{-8}	⋮	⋮	⋮
13	1.098×10^{-3}	3.721×10^{-7}	1.549×10^{-11}	1.548×10^{-11}	⋮	⋮	⋮
14	1.192×10^{-3}	5.689×10^{-8}			⋮	⋮	⋮
15	1.288×10^{-3}	5.707×10^{-9}			⋮	⋮	⋮
⋮	⋮				⋮	⋮	⋮
52	4.683×10^{-4}				⋮	⋮	1.890×10^{-4}
⋮	⋮				⋮	⋮	⋮
94	1.984×10^{-4}				3.788×10^{-4}	3.792×10^{-4}	1.875×10^{-8}
⋮	⋮				⋮	⋮	⋮
136	5.352×10^{-4}				⋮	⋮	1.137×10^{-11}
⋮	⋮				⋮	⋮	
178	4.431×10^{-4}				4.741×10^{-8}	7.098×10^{-8}	
⋮	⋮				⋮	⋮	
262	1.613×10^{-4}				6.765×10^{-12}	4.843×10^{-12}	
⋮	⋮						
4969	9.992×10^{-9}						

TABLE IV
COMPARISON BETWEEN CPU TIMES AND STABILITY IN CASE 2

Methods	CPU times (s)	Comparison between CPU times $\frac{T_{FB}}{T_{xx}}\big|_{xx=FB,...,EED}$	Max. Floquet multiplier
BF	76173.89	1.00	N/A
ND	4190.97	18.17	0.9978
FD	4170.62	18.26	N/A
DA	2285.46	33.32	0.9978
AT	2265.30	33.62	0.9978
END	2194.82	34.70	0.9989
DEE	1136.01	67.05	0.9975

A. Case study 3: Harmonic effects on the power quality

Table V presents a comparison between the root mean square (RMS) voltage, voltage ripple and total harmonic distortion (THD) of the bus voltages at Bus 1, Bus 2, Bus 4 and PCC of the steady state solution obtained with the DEE method and PSCAD, both with the detailed model (DM) and the simplified model (SM) of the controlled microgrid. The commutation of the VSCs is explicitly considered in the DM and only the fundamental component of the VSCs signals is taken into account in the SM approach.

According to Table V, the difference of the RMS voltage between the DEE method and PSCAD, in the worst case, is about 0.9 % and 0.0073 % for the detailed and the simplified

TABLE V
COMPARISON BETWEEN SOME SIGNALS OF THE SOLUTION OF DEE METHOD AND PSCAD.

	V_{RMS} (DEE-DM)	V_{RMS} (DEE-SM)	V_{RMS} (PSCAD-DM)	V_{RMS} (PSCAD-SM)	THD (DEE-DM)	THD (PSCAD-DM)	V_{Ripple} (DEE-DM)	V_{Ripple} (PSCAD-DM)
Bus 1	13.870 kV	13.8 kV	13.831 kV	13.8 kV	10.11%	11.10%	10.78%	12.11%
Bus 2	14.375 kV	13.8 kV	14.507 kV	13.8 kV	29.19%	31.90%	28.39%	28.71%
Bus 4	14.335 kV	13.8 kV	14.400 kV	13.8 kV	28.13%	30.60%	27.08%	27.79%
PCC	13.834 kV	13.732 kV	13.761 kV	13.731 kV	12.33%	12.25%	14.62%	15.04%

models, respectively. The results of the THD are close each others; however, the voltage ripples in percent of the peak voltage value of the detailed model have, in the worst case, a difference of 1.33 %. Please notice that the voltage signals at buses 1, 2, 4 and PCC have high THD; this harmonic distortion represents adverse effects in the microgrid operation, i.e., heating of conductors, premature aging of components, additional transmission losses, interference with communication and control systems, among others [35]. Regarding the additional losses, Table VI shows the total active power delivered by the VSCs at their AC terminals, the total active power consumed by the loads and the losses of the system both for the detailed and the simplified model, using the state space models and PSCAD. The power losses in Table VI do not include the ones in the VSCs, which in the best case could be around 2-5% of the delivered power. Additionally, Table VII presents a comparison between DG units in terms of apparent, active, reactive and distortion power. In this Table, it can be observed how the distortion power exceeds in all VSCs the reactive power, which in turn contributes to reach prematurely the current and power capacity of the power electronic converters leading to overrated operating conditions.

TABLE VI
ACTIVE POWER GENERATED, CONSUMED AND LOSSES.

	Simplified model (SSM)	Simplified model (PSCAD)	Detailed model (SSM)	Detailed model (PSCAD)
Generated power (P_{gen})	6.6942 MW	6.6940 MW	6.7296 MW	6.7015 MW
Consumed power (P_{cons})	6.6118 MW	6.6120 MW	6.6119 MW	6.5760 MW
Losses	82 kW	82 kW	117 kW	125 kW

B. Case study 4: Harmonic effects on the control performance

It was found that exist an interaction of the system and the closed-loop *dq* control implemented in the distributed generation units, so that 5th, 7th, 11th and 13th harmonics appear. Even though, all the odd harmonic components appear in the voltage and current waveforms of the microgrid (except triplen) with DGs based in SPWM VSCs, in practice is common to define the lowest order harmonic equal to $m_f - 2$, because it is expected that below this frequency the harmonic content is negligible.
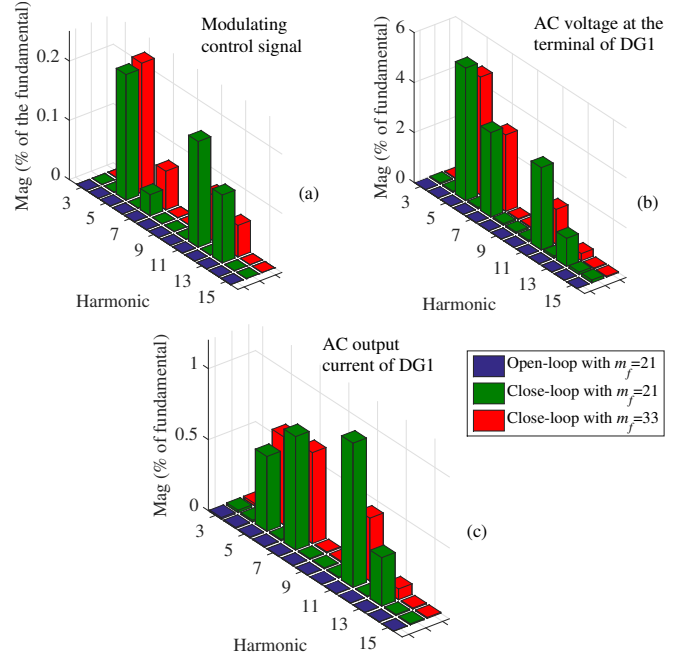

Fig. 4. Harmonic components for three different scenarios of the microgrid in autonomous mode, a) modulating control signal of the VSC (DG1), b) AC voltage at the terminal of DG1, c) AC output current of DG1. For the microgrid without control and $m_f = 21$, with close-loop control and $m_f = 33$, and with close-loop control and $m_f = 21$.

In order to evaluate the presence of the 5th, 7th, 11th and 13th harmonics with the closed-loop control operation, please consider that Fig. 4(a) shows the modulating control signal spectrum of DG1, Fig. 4(b) shows the AC voltage spectrum at the terminal of DG1, and Fig. 4(c) shows the AC current spectrum of DG1 under three different scenarios: open-loop control and $m_f = 21$, closed-loop control with $m_f = 21$, and closed-loop control with $m_f = 33$. Notice that without interaction between the microgrid measurements and the control action (open-loop control), the 5th, 7th, 11th and 13th components vanished. On the other hand, with closed-loop control, the 5th, 7th, 11th and 13th harmonics appear with significant values. It is important to notice that their magnitude do not decrease inversely with m_f as is shown in Fig. 4 with $m_f = 21$ and $m_f = 33$. Actually, in Fig. 4(a), the harmonics 5th and 7th increase their magnitude for $m_f = 33$ as compared with those obtained with $m_f = 21$.

The nonlinear operations in controllers using distorted signals obtained from measurements derive in harmonic cross-

TABLE VII
COMPARISON BETWEEN DG UNITS IN TERMS OF APPARENT, ACTIVE, REACTIVE AND DISTORTION POWER.

	Apparent power (S)	Active power (P)	Reactive power (Q)	Distortion power (D)
DG1	2.6776 MVA	1.9842 MW	0.7775 MVAr	1.6211 MVAd
DG2	2.3391 MVA	1.7712 MW	0.7452 MVAr	1.3337 MVAd
DG3	3.9694 MVA	2.9741 MW	1.0402 MVAr	2.4143 MVAd

coupling [36], which tie the entire harmonic spectrum, so that the high order harmonic are mapped into the low order harmonics. In addition, previous contributions have exposed that harmonic interactions phenomena arise in controlled microgrids; however, they have not been still fully explored and understood [1], [9], [13], [37].

Therefore, the inherent harmonic cross-coupling, the resonances of the system and the interaction among the network, the control and the power electronic devices, lead to the apparition of non-characteristic harmonic components which are supposed to not exist. In this way, Fig. 5 shows the magnitude of the low order harmonics of the control signal for different m_f.
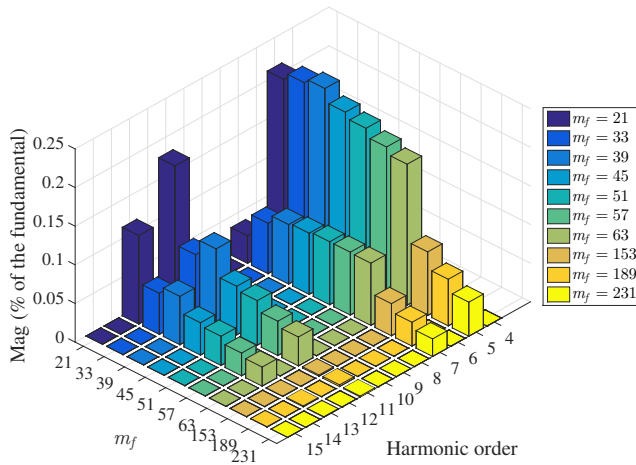

Fig. 5. Harmonic components of the modulating control signal using different m_f.

Observe in Fig. 5 that the low order harmonics in the control signal have a non-characteristic behavior, that is, the magnitudes of the harmonic components oscillate as the switching frequency increases up to $m_f = 39$ (2.34 kHz), above this switching frequency the harmonic components asymptotically decreases as f_{sw} increases, as commonly expected. Despite the spectrum magnitude of the control signal could be considered negligible, it has a significant impact on the electrical variables of microgrid as shown in Fig. 4 (b) and (c), and in this case leads to unacceptable level of some harmonic components [38].

Please note that if detailed models of the system components and explicit consideration of the control system are not used, similar interactions to those found in this study can

be overlooked in the design and evaluation stages leading to implementation issues. Further research is needed in this specific topic.

C. Case study 5: Harmonic effects on the asymptotic stability

In practical microgrids, the DG units commonly have different switching frequencies, typically according to their nominal capacity, furthermore, the equivalent impedance at the PCC looking towards the main grid can change at any time depending on many external factors, such as network reconfiguration, load change, among others. Regarding to the above, in this case study a variation of the short circuit capacity (SCC) of the main grid is carried out in order to analyze the steady state behavior of the MG (SCC$\in$ (30 : 2000) MVA), additionally, the m_f of DG1, DG2 and DG3 is 27, 27 and 15, respectively; the capacitor bank capacity is changed to 2.5 MVAr for a proper performance in the nominal operation point. The nominal SCC of the grid at PCC is 926 MVA.
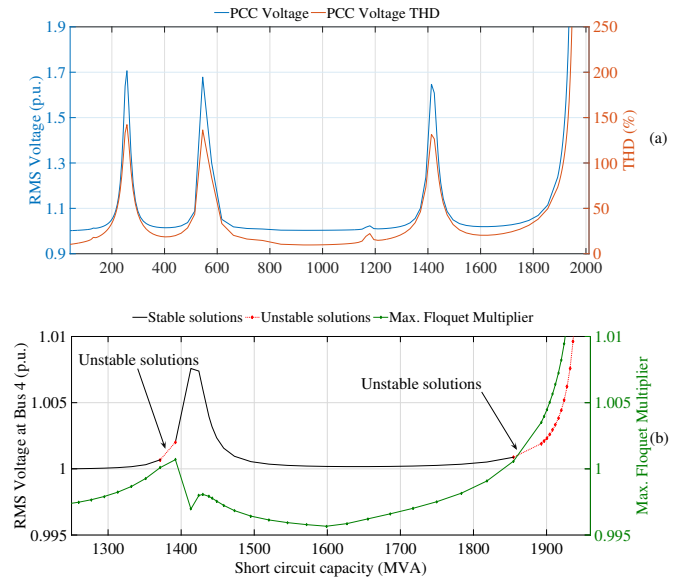

Fig. 6. (a) RMS and THD of the PCC voltage; (b) RMS voltage of Bus 4 and the maximum Floquet multiplier of the system. Stable solutions are plotted with continuous line and unstable solutions with dot marked line.

Figure 6(a) shows the RMS in per unit (p.u.) and the THD of the PCC voltage, and Fig. 6(b) shows the RMS voltage in p.u. of the Bus 4 and the maximum Floquet multiplier of the system showing the stable solutions with continuous line and the unstable solutions with dot markers. Parallel resonances

arise in some values of SCC, and these resonances provoke an increase of the THD and RMS magnitude of the PCC voltage, as shown in Fig. 6(a); in the worst case the THD increases up to 142.4 %, and the RMS voltage up to 1.7 p.u., furthermore, for SCC above 1800 MVA the system becomes unstable and collapses. Despite the PCC voltage increases its magnitude due to the resonances, the magnitude of the controlled bus voltages (buses 1, 2 and 4) remain close to 1 p.u., being 1.03 p.u. the worst stable case, as per Fig. 6(b).

On the other hand, observe that the system loses stability when the SCC is within 1350 MVA and 1392 MVA. It should also be mentioned that using the fundamental frequency model, the system remains stable over the full range of variation and the RMS voltages in all buses have no variations. Although the fundamental frequency model does not preserve the information of the resonances, we expect that it holds the information about the stability; however, in this case study is corroborated that in systems such as microgrids, the stability can not be computed accurately using only fundamental frequency models due to the phenomena presented in the real system, such as resonances and the interactions between the control and the rest of the MG components.

Figure 7 shows the spectrum of the modulating control signal of DG1, the AC terminal voltage of DG1 and the AC output current of DG1, when the SCC is 225 MVA (see Fig. 6(a)). Please notice that, due to the resonances in the system, low frequency harmonics that not appear using the fundamental frequency model (as can be seen in Section VI-B), increase their magnitude up to prohibitive values [38] which, in turn, could lead to an improper operation of the MG.
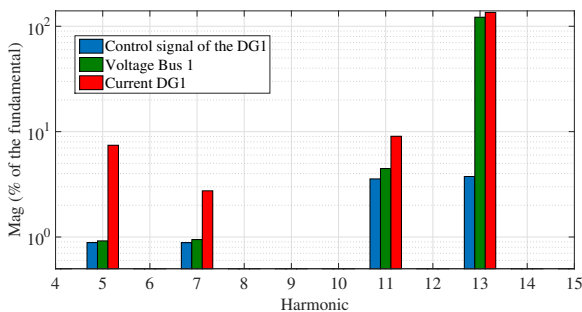

Fig. 7. Harmonic content of the modulating control signal of the DG1, the voltage of Bus 1 and the current of DG1, when the system is in a peak of resonance (SCC 225 MVA).

It is important to notice that to analyze all the dynamics that appear in the system and, moreover, to obtain solutions more reliable in steady state studies, detailed models of the components and efficient mathematical methods are required, and by virtue of this the fast-time domain methods for the computation of the periodic steady state solution and stability are presented in this work.

VII. CONCLUSION

A complete scenario for a microgrid, considering multiple aspects such as, harmonics, nonlinearities, closed-loop controls and stability were established to compare seven time-domain methods: six Newton-type methods and the so called brute force approach. The results reveal the issues and the importance of considering detailed microgrid models for steady state analysis.

The presented Newton methods exceed the BF method in all cases in terms of CPU time. The DEE method was the fastest, although the one with the worst convergence rate per iteration. Nevertheless, the DEE method was 67 and 68 times faster than BF method in the worst and best case, respectively. In addition, the AT, ND, DA, END, and DEE methods, give accurately the associated stability of the computed limit cycle. All Newton methods can compute stable and unstable solutions.

In order to show the potential applications of the Newton methods in detailed microgrid studies, basic case studies on harmonic analysis were conducted to show the adverse effects of the harmonic distortion on power quality, losses, control performance and stability. On the other hand, the obtained results confirm that for stressed and harmonic distorted scenarios is necessary to consider explicitly the commutation process of the power electronic devices and the control systems in order to not overlook phenomena or undesirable behaviors of the system. Therefore, the Newton methods are an outstanding and straightforward alternative for harmonic stability and power quality analysis since allow the use of full state-space models including the complete representation of the control systems and the explicit consideration of the commutation process of the power electronic converters without resort to unnecessary simplification that compromise the reliability in the analyses.

REFERENCES

[1] X. Tang, W. Deng, and Z. Qi, "Investigation of the dynamic stability of microgrid," *Power Systems, IEEE Transactions on*, vol. 29, no. 2, pp. 698–706, March 2014.

[2] M. M. Hashempour, M. Savaghebi, J. C. Vasquez, and J. M. Guerrero, "Hierarchical control for voltage harmonics compensation in multi-area microgrids," in *Diagnostics for Electrical Machines, Power Electronics and Drives (SDEMPED), 2015 IEEE 10th International Symposium on*, Sept 2015, pp. 415–420.

[3] I. Lorzadeh, H. Abyaneh, M. Savaghebi, and J. Guerrero, "A hierarchical control scheme for reactive power and harmonic current sharing in islanded microgrids," in *Power Electronics and Applications (EPE'15 ECCE-Europe), 2015 17th European Conference on*, Sept 2015, pp. 1–10.

[4] S. Acevedo and M. Molinas, "Power electronics modeling fidelity: Impact on stability estimate of micro-grid systems," in *Innovative Smart Grid Technologies Asia (ISGT), 2011 IEEE PES*, Nov 2011, pp. 1–8.

[5] D. Olivares, A. Mehrizi-Sani, A. Etemadi, C. Canizares, R. Iravani, M. Kazerani, A. Hajimiragha, O. Gomis-Bellmunt, M. Saeedifard, R. Palma-Behnke, G. Jimenez-Estevez, and N. Hatziargyriou, "Trends in microgrid control," *IEEE Transactions on Smart Grid*, vol. 5, no. 4, pp. 1905–1919, Jul. 2014.

[6] S. Dasgupta, S. Mohan, S. Sahoo, and S. Panda, "Lyapunov function-based current controller to control active and reactive power flow from a renewable energy source to a generalized three-phase microgrid system," *IEEE Transactions on Industrial Electronics*, vol. 60, no. 2, pp. 799–813, Feb. 2013.

[7] J. Peas Lopes, C. Moreira, and A. Madureira, "Defining control strategies for microgrids islanded operation," *Power Systems, IEEE Transactions on*, vol. 21, no. 2, pp. 916–924, May 2006.

[8] N. Eghtedarpour and E. Farjah, "Power control and management in a hybrid ac/dc microgrid," *Smart Grid, IEEE Transactions on*, vol. 5, no. 3, pp. 1494–1505, May 2014.

[9] X. Wang, F. Blaabjerg, and W. Wu, "Modeling and analysis of harmonic stability in an ac power-electronics-based power system," *Power Electronics, IEEE Transactions on*, vol. 29, no. 12, pp. 6421–6432, Dec 2014.

[10] "Conditions for stability of droop-controlled inverter-based microgrids," *Automatica*, vol. 50, no. 10, pp. 2457 – 2469, 2014.

[11] J. Segundo-Ramirez, E. Barcenas, A. Medina, and V. Cardenas, "Steady-state and dynamic state-space model for fast and efficient solution and stability assessment of asds," *Industrial Electronics, IEEE Transactions on*, vol. 58, no. 7, pp. 2836–2847, July 2011.

[12] J. Segundo-Ramirez, A. Medina, A. Ghosh, and G. Ledwich, "Stability boundary analysis of the dynamic voltage restorer in weak systems with dynamic loads," *International journal of circuit theory and applications*, vol. 40, no. 6, pp. 551–569, 2012.

[13] F. Wang, J. Duarte, M. Hendrix, and P. Ribeiro, "Modeling and analysis of grid harmonic distortion impact of aggregated dg inverters," *Power Electronics, IEEE Transactions on*, vol. 26, no. 3, pp. 786–797, March 2011.

[14] D. Olivares, A. Mehrizi-Sani, A. Etemadi, C. Canizares, R. Iravani, M. Kazerani, A. Hajimiragha, O. Gomis-Bellmunt, M. Saeedifard, R. Palma-Behnke, G. Jimenez-Estevez, and N. Hatziargyriou, "Trends in microgrid control," *Smart Grid, IEEE Transactions on*, vol. 5, no. 4, pp. 1905–1919, July 2014.

[15] T. Parker and L. Chua, *Practical Numerical Algorithms for Chaotic Systems*. Springer London, Limited, 2011.

[16] H. Dommel, "Digital computer solution of electromagnetic transients in single-and multiphase networks," *IEEE Transactions on Power Apparatus and Systems*, vol. PAS-88, no. 4, pp. 388–399, April 1969.

[17] S. Banerjee and G. Verghese, *Nonlinear Phenomena in Power Electronics: Bifurcations, Chaos, Control, and Applications*. Wiley, 2001.

[18] J. Martinez-Velasco, *Transient Analysis of Power Systems: Solution Techniques, Tools and Applications*, ser. Wiley - IEEE. Wiley, 2015.

[19] R. Peña, J. Núñez, and A. Medina, "Using a newton method and LAPACK libraries to initialize electromagnetic transient simulations in power systems," *Simulation Modelling Practice and Theory*, vol. 42, pp. 12–18, Mar. 2014.

[20] A. Medina, J. Segundo, P. Ribeiro, W. Xu, K. Lian, G. Chang, V. Dinavahi, and N. Watson, "Harmonic analysis in frequency and time domain," *IEEE Transactions on Power Delivery*, vol. 28, no. 3, pp. 1813–1821, July 2013.

[21] T. Aprille and T. Trick, "A computer algorithm to determine the steady-state response of nonlinear oscillators," *IEEE Transactions on Circuit Theory*, vol. 19, no. 4, pp. 354–360, 1972.

[22] J. Aprille, T.J. and T. N. Trick, "Steady-state analysis of nonlinear circuits with periodic inputs," *Proceedings of the IEEE*, vol. 60, no. 1, pp. 108–114, Jan 1972.

[23] A. Nayfeh and B. Balachandran, *Applied Nonlinear Dynamics: Analytical, Computational and Experimental Methods*, ser. Wiley Series in Nonlinear Science. Wiley, 2008.

[24] A. Semlyen and A. Medina, "Computation of the periodic steady state in systems with nonlinear components using a hybrid time and frequency domain methodology," *IEEE Transactions on Power Systems*, vol. 10, no. 3, pp. 1498–1504, Aug 1995.

[25] J. Segundo-Ramírez and A. Medina, "An enhanced process for the fast periodic steady state solution of nonlinear systems by Poincaré map and extrapolation to the limit cycle," *International Journal of Nonlinear Sciences and Numerical Simulation*, vol. 11, no. 8, pp. 661–670, Aug 2010.

[26] ——, "computation of the steady state solution of nonlinear power systems by extrapolation to the limit cycle using a discrete exponential expansion method," *International Journal of Nonlinear Sciences and Numerical Simulation*, vol. 11, no. 8, pp. 655–660, Aug 2010.

[27] "IEEE recommended practice for industrial and commercial power system analysis," *IEEE Std 399-1990*, pp. 1–384, Dec 1990.

[28] F. Katiraei and M. Iravani, "Power management strategies for a microgrid with multiple distributed generation units," *IEEE Transactions on Power Systems*, vol. 21, no. 4, pp. 1821–1831, Nov 2006.

[29] F. Katiraei, M. Iravani, and P. Lehn, "Micro-grid autonomous operation during and subsequent to islanding process," *IEEE Transactions on Power Delivery*, vol. 20, no. 1, pp. 248–257, Jan 2005.

[30] ——, "Small-signal dynamic model of a micro-grid including conventional and electronically interfaced distributed resources," *IET Generation, Transmission and Distribution*, vol. 1, no. 3, pp. 369–378, May 2007.

[31] J. Segundo-Ramirez and A. Medina, "Modeling of FACTS devices based on SPWM VSCs," *IEEE Transactions on Power Delivery*, vol. 24, no. 4, pp. 1815–1823, Oct 2009.

[32] H. Manitoba, "Research centre," *PSCAD/EMTDC: Electromagnetic transients program including dc systems*, 1994.

[33] H. Dommel, *EMTP Theory Book*. Microtran Power System Analysis Corporation, 1996.

[34] J. H. R. Enslin and P. J. M. Heskes, "Harmonic interaction between a large number of distributed power inverters and the distribution network," in *Power Electronics Specialist Conference, 2003. PESC '03. 2003 IEEE 34th Annual*, vol. 4, June 2003, pp. 1742–1747 vol.4.

[35] S. Chowdhury and P. Crossley, *Microgrids and Active Distribution Networks*, ser. IET renewable energy series. Institution of Engineering and Technology, 2009.

[36] J. Rico, M. Madrigal, and E. Acha, "Dynamic harmonic evolution using the extended harmonic domain," *Power Delivery, IEEE Transactions on*, vol. 18, no. 2, pp. 587–594, April 2003.

[37] T. Green and M. Prodanovi, "Control of inverter-based micro-grids," *Electric Power Systems Research*, vol. 77, no. 9, pp. 1204 – 1213, 2007, distributed Generation.

[38] A. Rockhill, M. Liserre, R. Teodorescu, and P. Rodriguez, "Grid-filter design for a multimegawatt medium-voltage voltage-source inverter," *Industrial Electronics, IEEE Transactions on*, vol. 58, no. 4, pp. 1205–1217, April 2011.